

Resonance structure of ${}^8\text{Be}$ with the two-cluster resonating group method

V. O. Kurmangaliyeva¹, N. Kalzhigitov¹, N. Zh. Takibayev¹,
V. S. Vasilevsky²

¹Al-Farabi Kazakh National University, Almaty, Kazakhstan

²Bogolyubov Institute for Theoretical Physics, Kiev, Ukraine

April 23, 2022

Abstract

A two-cluster microscopic model is applied to study elastic alpha-alpha scattering and resonance structure of ${}^8\text{Be}$. The model is an algebraic version of the Resonating Group Method, which makes use complete set of oscillator functions to expand wave function of two-cluster system. Interaction between clusters is determined by well-known semi-realistic nucleon-nucleon potentials of Hasegawa-Nagata, Minnesota and Volkov. Detail analysis of resonance wave functions is carried out in oscillator, coordinate and momentum spaces. Effects of the Pauli principle on wave functions of the ${}^8\text{Be}$ continuous spectrum states are thoroughly studied.

1 Introduction

Nucleus ${}^8\text{Be}$ is a very interesting object which attracts large attention from various theoretical and experimental methods. This nucleus has no bound states but it has a rich collection of resonance states. The low-energy part of resonance states belongs to the two-cluster continuum of two interacting alpha particles. There are three resonance states 0^+ , 2^+ and 4^+ , which are considered as a rotational band of the ${}^8\text{Be}$ nucleus. The 0^+ resonance state is a very narrow resonance state with the energy 0.092 MeV above the $\alpha + \alpha$ decay threshold. The width of this state is 5.57 eV and the half-life time is 8.19×10^{-17} seconds [1]. This allows one to treat it approximately as a bound state. As the threshold energy of the second channel $p+{}^7\text{Li}$ is 17.35 MeV with respect to the energy of the first channel, then the $\alpha + \alpha$ channel is dominant in a wide energy range ($0 \leq E \leq 15$ MeV).

In the present paper we are going to study structure of ${}^8\text{Be}$ and pay main attention to wave functions of resonance states. For this aim we employ a specific variant (version) of the resonating group method (RGM) which was formulated in Refs. [2, 3] and is known as the algebraic version of the resonating group method. The key element of the algebraic version is that it uses wave functions of three-dimension harmonic oscillator to expand wave functions of inter-cluster motion and thus it realizes a matrix form of quantum mechanical description of nuclear system. The matrix form can be applied to study both bound and resonance states since corresponding boundary conditions well-known in coordinate space were transformed into discrete, oscillator representation. At present time, the algebraic version of the resonating group method is very efficient and popular tool to study dynamics of two-cluster systems ([4, 5, 6, 7, 8]), and three-cluster systems as well ([9, 10, 11, 12]).

The present paper is a continuation of the investigations of ${}^8\text{Be}$ started in Ref. [7]. In the present paper we will reveal new interesting information on peculiarities of dynamics of two-cluster systems and their manifestations in ${}^8\text{Be}$. We discuss different ways of detecting resonance states and we show how resonance states affect behavior of a numerous number of observable (partial and total cross section of elastic scattering and so on) and non-observable (wave function, an average distance between clusters and so on) physical quantities. As our model involves oscillator basis, we then analyze behavior of wave functions in oscillator, coordinate and momentum representations. An explicit evidence of a simple relation between expansion coefficients and corresponding wave function in coordinate space will be shown for a continuous spectrum state.

The layout of the present paper is the following. In Sec. 2 we shortly review principal ideas of the two-cluster model. In this section we also introduce all necessary quantities which will be used to analyze obtained results. Sec. 3 will start with selecting of nucleon-nucleon potentials and with fixing all input parameters of our calculations. Then it proceeds with analysis of phase shifts of elastic alpha-alpha scattering and determination of the energy and width of resonance states. After that, peculiarities of wave functions of resonance states and effects of the Pauli principle on continuous spectrum states of ${}^8\text{Be}$ are discussed in detail. The final section summarizes main results of our investigations.

2 Method

Formulation of a microscopic method requires to display many-particle Hamiltonian and an explicit form of wave function. Hamiltonian which will be used in our calculations involves the kinetic energy operator, a semi-realistic nucleon-nucleon potential and the Coulomb interaction of protons. To achieve our goals, the sought wave function is selected to reproduce two-cluster structure of ${}^8\text{Be}$. Therefore, wave function of ${}^8\text{Be}$ comprised of two alpha particles

is represented in the form

$$\Psi_{EL} = \widehat{\mathcal{A}} \{ \Phi_1 ({}^4\text{He}, b) \Phi_2 ({}^4\text{He}, b) \psi_{EL}(q) Y_{LM}(\widehat{\mathbf{q}}) \}, \quad (1)$$

where $\widehat{\mathcal{A}}$ is the antisymmetrization operator, $\Phi_1 ({}^4\text{He}, b)$ and $\Phi_2 ({}^4\text{He}, b)$ are the translational invariant and antisymmetric functions describing internal structure of the first and second alpha clusters, respectively. Since spin of an alpha particle equals zero, then the total spin S of ${}^8\text{Be}$ equals also zero and therefore the total angular momentum J coincides with the total orbital momentum L . Throughout of the text we will use the total orbital momentum L to mark different rotation states of ${}^8\text{Be}$. A wave function $\psi_{EL}(q)$ represents radial motion two clusters, while the spherical harmonic $Y_{LM}(\widehat{\mathbf{q}})$ represents rotating motion of clusters. The Jacobi vector $\mathbf{q} = q \cdot \widehat{\mathbf{q}}$ ($\widehat{\mathbf{q}}$ is a unit vector orientation of which in space is fixed by two angles θ_q and ϕ_q) is proportional to the distance \mathbf{r} between interacting clusters

$$\mathbf{q} = \mathbf{r} \sqrt{\frac{A_1 A_2}{A_1 + A_2}} = \sqrt{\frac{A_1 A_2}{A_1 + A_2}} \left[\frac{1}{A_1} \sum_{i \in A_1} \mathbf{r}_i - \frac{1}{A_2} \sum_{j \in A_2} \mathbf{r}_j \right], \quad (2)$$

where $\mathbf{r}_1, \mathbf{r}_2, \dots, \mathbf{r}_A$ are coordinates in the space of individual nucleons.

The main assumption of the RGM is that wave functions $\Phi_1 ({}^4\text{He}, b)$ and $\Phi_2 ({}^4\text{He}, b)$ are known and fixed, while the inter-cluster function $\psi_{EL}(q)$ has to be obtained by solving the dynamic equations. In the standard version of the RGM, one has to solve the integro-differential equation. The integral or nonlocal part of the equation appears due to the antisymmetrization operator or, in other words, due to the Pauli principle. In the algebraic version of RGM, the dynamic equations transforms in to a set of linear algebraic equations. This is achieved by using a full set of the radial part of oscillator functions $\{\Phi_{nL}(q, b)\}$. By expanding the inter-cluster function $\psi_{EL}(q)$ over oscillator functions

$$\psi_{EL}(q) = \sum_{n=0}^{\infty} C_{nL}^{(E)} \Phi_{nL}(q, b) \quad (3)$$

or the total two-cluster function Ψ_{EL} over cluster oscillator functions $\{|nL\rangle\}$

$$\Psi_{EL} = \sum_{n=0}^{\infty} C_{nL}^{(E)} |nL\rangle, \quad (4)$$

we arrive to a system of linear algebraic equations

$$\sum_{\tilde{n}=0}^{\infty} \left\{ \langle nL | \widehat{H} | \tilde{n}L \rangle - E \delta_{n\tilde{n}} \Lambda_{nL} \right\} C_{\tilde{n}L}^{(E)} = 0. \quad (5)$$

The cluster oscillator function is determined as

$$|nL\rangle = \widehat{\mathcal{A}} \{ \Phi_1(^4\text{He}, b) \Phi_2(^4\text{He}, b) \Phi_{nL}(q, b) Y_{LM}(\widehat{\mathbf{q}}) \}. \quad (6)$$

One can see that an oscillator function $\Phi_{nL}(q, b)$ describes relative motion of two alpha particles in the cluster function (6). And here is the explicit form of the oscillator function

$$\begin{aligned} \Phi_{nL}(q, b) &= (-1)^n \mathcal{N}_{nL} b^{-3/2} \rho^L e^{-\frac{1}{2}\rho^2} L_n^{L+1/2}(\rho^2), \\ \rho &= q/b. \end{aligned} \quad (7)$$

As we interested in the inter-cluster wave function in the momentum space $\psi_{EL}(p)$, we present also oscillator functions in momentum space

$$\begin{aligned} \Phi_{nL}(p, b) &= \mathcal{N}_{nL} b^{3/2} \rho^L e^{-\frac{1}{2}\rho^2} L_n^{L+1/2}(\rho^2), \\ \rho &= p \cdot b, \end{aligned} \quad (8)$$

where

$$\mathcal{N}_{nL} = \sqrt{\frac{2\Gamma(n+1)}{\Gamma(n+L+3/2)}}$$

and $L_n^\alpha(z)$ is the generalized Laguerre polynomial [13].

The system of equations (5) contains matrix elements of Hamiltonian between cluster oscillator functions $\langle nL | \widehat{H} | \tilde{n}L \rangle$ and matrix elements of unit operator $\langle nL | \tilde{n}L \rangle$. For two-cluster systems, matrix elements are diagonal with respect to quantum numbers n and \tilde{n} and coincides with the so-called eigenvalues of the norm kernel Λ_{nL}

$$\langle nL | \tilde{n}L \rangle = \delta_{n, \tilde{n}} \Lambda_{nL}.$$

For ^8Be the eigenvalues Λ_{nL} equal

$$\Lambda_{nL} = \frac{1}{2} \sum_{k=0}^4 \frac{4! (-1)^k}{k! (4-k)!} \left[1 - k \frac{1}{2} \right]^{2n+L}. \quad (9)$$

The system of equations (5) is deduced directly from the Schrödinger equation

$$\left(\widehat{H} - E \right) \Psi_{EL} = 0$$

for the wave function (1).

By solving the set of equations (5), one obtains the energy and a wave function of bound states, or a wave function and the scattering S -matrix for continuous spectrum states. If in Eq. (5) we restrict ourselves with a finite number (we denote it N) of oscillator function ($n=0, 1, \dots, N-1$), we encounter the generalized eigenvalue problem for $N \times N$ matrices. By solving this problem, we obtain the energy spectrum E_ν ($\nu=1, 2, \dots, N$) and wave functions $\{C_{nL}^{(E_\nu)}\}$ of bound and pseudo-bound states. The latter are continuous spectrum states describing alpha-alpha scattering states with specific conditions. It was shown in Ref. [14] that the wave functions of pseudo-bound states in oscillator space has a node at the point N , i.e.

$$C_{NL}^{(E_\nu)} = 0.$$

Thus, diagonalization of Hamiltonian with a fixed number of oscillator functions selects from continuous spectrum states those states which obey specific boundary condition.

To solve the system of equations (1) for a scattering state, one has to formulate proper boundary conditions in discrete oscillator space and then incorporate them in a set of equations (5). This problem has been numerously discussed in literature (see, for instance, [15], [16] [2], [3], [17]). Here we shortly outline practical steps to obtain and analyze scattering states.

In oscillator space like in coordinate space, we split the space on two parts or two regions: internal and asymptotic regions. Let us recall how boundary conditions are formulated and used in coordinate space. In the internal region interaction between clusters are prominent and it should be treated correctly. In the asymptotic region interaction between clusters originated from a short-range nucleon-nucleon potential is negligibly small, and can therefore be ignored. In consequence of this fact, in the asymptotic region Hamiltonian consists of the kinetic energy operator \hat{T}_q of relative motion of clusters for neutral clusters (or when one of the clusters is a neutron), for charged clusters it consists of the same kinetic energy operator and the Coulomb interaction of two point-like charged particles

$$\hat{H} = \hat{T}_q + \frac{Z_1 Z_2 e^2}{q} \sqrt{\mu}, \quad (10)$$

Where $Z_1(Z_2)$ is a charge of the first (second) cluster, $e^2 = 1.44 \text{ MeV}\cdot\text{fm}$ is the square of the elementary charge in nuclear units, and

$$\begin{aligned} \hat{T}_q &= -\frac{\hbar^2}{2m} \left[\frac{d^2}{dq^2} + 2\frac{1}{q} \frac{d}{dq} - \frac{L(L+1)}{q^2} \right], \\ \mu &= \frac{A_1 A_2}{A_1 + A_2}. \end{aligned} \quad (11)$$

It is well-known (see, for example, books [18], [19]) that Hamiltonian (10) has two independent solutions

$$\psi_{kL}^{(R)}(q) = \sqrt{\frac{2}{\pi}} k \frac{F_L(\rho, \eta)}{\rho}, \quad \psi_{kL}^{(I)}(q) = \sqrt{\frac{2}{\pi}} k \frac{G_L(\rho, \eta)}{\rho}, \quad (12)$$

where $\rho = kq$, η is the Sommerfeld parameter:

$$\eta = \frac{Z_1 Z_2 e^2}{\hbar k} \sqrt{\mu m}. \quad (13)$$

Wave functions $\psi_{kL}^{(R)}(q)$ and $\psi_{kL}^{(I)}(q)$ describes scattering of charged particles and are regular and irregular (singular) at the origin of coordinates. For neutral particles, when $\eta = 0$, these functions are the spherical Bessel and Neumann functions

$$\psi_{kL}^{(R)}(q) = \sqrt{\frac{2}{\pi}} k j_L(\rho), \quad \psi_{kL}^{(I)}(q) = -\sqrt{\frac{2}{\pi}} k n_L(\rho, \eta), \quad (14)$$

General solutions of Hamiltonian (10) is the following combination of regular and irregular functions

$$\psi_{kL}^{(a)}(q) = \psi_{kL}^{(R)}(q) + \tan \delta_L \psi_{kL}^{(I)}(q), \quad (15)$$

where δ_L is a phase shift of elastic cluster-cluster scattering. If we managed to calculate the phase shift δ_L , then we immediately determine two-cluster wave function in semi-infinite range of distances $R_i \leq q < \infty$, where R_i indicates the inter-cluster distance which marks a border between the internal and asymptotic regions. Eq. (15) explicitly demonstrate boundary conditions for scattering states in a single-channel case. The asymptotic wave function $\psi_{kL}^{(a)}(q)$ at the point $q = R_i$ has to be matched with the internal wave function $\psi_{kL}^{(i)}(q)$, which we assume is determined by numerical solution of the Schrödinger equation in the range of inter-cluster distances $0 \leq q < R_i$. The boundary conditions then are read as

$$\psi_{kL}^{(i)}(R_i) = \psi_{kL}^{(a)}(R_i), \quad (16)$$

$$\left. \frac{d}{dq} \psi_{kL}^{(i)}(q) \right|_{q=R_i} = \left. \frac{d}{dq} \psi_{kL}^{(a)}(q) \right|_{q=R_i}, \quad (17)$$

where the asymptotic and internal wave functions are matched and their first derivatives as well. These conditions guarantee that the inter-cluster wave function and its first derivative are continuous at the point $q = R_i$.

Essentially the same ideas were used to formulate boundary in oscillator representations. Here we present the shortest way of explanation but not completely rigorous. For the sake of

simplicity, we consider neutral clusters. As we pointed out above, Hamiltonian in asymptotic region consists of the kinetic energy operator. In oscillator representation, this Hamiltonian has a tridiagonal or Jacobi matrix form. Nonzero matrix elements $\langle m, L | \hat{T}_q | n, L \rangle$ of the kinetic energy operator are

$$\langle mL | \hat{T}_q | nL \rangle = \frac{\hbar^2}{2mb^2} \begin{cases} -\sqrt{n(n+L+\frac{1}{2})} & m = n-1 \\ (2n+L+\frac{3}{2}) & m = n \\ -\sqrt{(n+1)(n+L+\frac{3}{2})} & m = n+1 \end{cases} . \quad (18)$$

It was shown in Refs. [16], [20], [21] that the matrix equation

$$\sum_{n=0}^{\infty} [\langle mL | \hat{T}_q | nL \rangle - E\delta_{mn}] C_{nL} = 0 \quad (19)$$

has two independent solutions $C_{nL}^{(R)}(kb)$ and $C_{nL}^{(I)}(kb)$, traditionally we refer to them as to regular and irregular solutions of the equations (19). Explicit form of the solutions $C_{nL}^{(R)}(kb)$ and $C_{nL}^{(I)}(kb)$ can be found in Ref. [16], [20], [21]. It was shown in Refs. [2], [3] that for large values of n the expansion coefficients $C_{nL}^{(R)}(kb)$ and $C_{nL}^{(I)}(kb)$ are connected to the regular and irregular functions (14) by the simple relations

$$C_{nL}^{(R)}(kb) \approx \sqrt{2R_n} \psi_{kL}^{(R)}(R_n), \quad C_{nL}^{(I)}(kb) \approx \sqrt{2R_n} \psi_{kL}^{(I)}(R_n), \quad (20)$$

where

$$R_n = b\sqrt{4n+L+3} \quad (21)$$

is the turning point of the classical harmonic oscillator. The relations (20) reflect general properties of oscillator functions. To this end, relations similar to (20) are valid for any functions of a two-cluster system and corresponding expansion coefficients. It was explicitly demonstrated in Ref. [22] for the wave function of the ${}^6\text{Li}$ ground state. It was shown that the relation between wave function and expansion coefficients (20) is valid even for small values of n ($n \geq 5$). In present calculations we use similar relations for the expansion coefficients of the asymptotic wave functions (12) for charged clusters.

To solve Eq. (5) for continuous spectrum states, we have to introduce appropriate boundary conditions in that set of equations. For this aim an infinite set of expansion coefficients is divided on two subsets - internal and asymptotic:

$$\left\{ C_{nL}^{(E)} \right\} = \left\{ C_{0L}^{(E)}, C_{1L}^{(E)}, \dots, C_{N-1L}^{(E)}, C_{\nu L}^{(R)} + \tan \delta_L C_{\nu L}^{(I)} \right\}, \quad (22)$$

where index ν ($N \leq \nu < \infty$) numerates expansion coefficients in the asymptotic region. With such form of expansion coefficients we have got $N + 1$ unknown quantities (N expansion coefficients in internal region and phase shift δ_L) to be determined. By substituting the expansion coefficients (22) in Eq. (5), we obtain

$$\begin{aligned} & \sum_{\tilde{n}=0}^{N-1} \left\{ \langle nL | \hat{H} | \tilde{n}L \rangle - E \langle nL | \tilde{n}L \rangle \right\} C_{nL}^{(E)} + \tan \delta_L \sum_{\nu \geq N} \langle nL | \hat{H} | \nu L \rangle C_{\nu L}^{(I)} \\ & = - \sum_{\nu \geq N} \langle nL | \hat{H} | \nu L \rangle C_{\nu L}^{(R)}. \end{aligned} \quad (23)$$

It is important to underline that in this system of equations, index n is run from 0 to $N - 1$, and thus we have a set of $N + 1$ linear algebraic equations for $N + 1$ unknown quantities. By taking into account Eq. (19), we can simplify the set of equations (23)

$$\begin{aligned} & \sum_{\tilde{n}=0}^{N-1} \left\{ \langle nL | \hat{H} | \tilde{n}L \rangle - E \langle nL | \tilde{n}L \rangle \right\} C_{nL}^{(E)} + \tan \delta_L \sum_{\nu \geq N} \langle nL | \hat{V} | \nu L \rangle C_{\nu L}^{(I)} \\ & = - \sum_{\nu \geq N} \langle nL | \hat{V} | \nu L \rangle C_{\nu L}^{(R)}. \end{aligned} \quad (24)$$

This is basic set of equations which allows us to obtain a phase shift and wave function of continuous spectrum states. Numerical solution of this set of equations is performed with a finite sum of index ν , in our calculations presented bellow the sum involves 20 terms.

We will not also dwell on calculating of matrix elements of the kinetic and potential energy operators, as their explicit form and reliable methods of their calculations can be found in Ref. [17].

It is important to note that wave function Ψ_{EL} for bound and pseudo-bound states is traditionally normalized to unit

$$\langle \Psi_{EL} | \Psi_{EL} \rangle = \sum_{n=0}^{\infty} |C_{nL}^{(E)}|^2 = 1,$$

however, corresponding inter-cluster function is normalized as

$$\langle \psi_{EL} | \psi_{EL} \rangle = S_L. \quad (25)$$

In oscillator representation it can be represented as

$$S_L = \sum_{n=0}^{\infty} |C_{nL}^{(E)}|^2 / \lambda_n \quad (26)$$

The quantity S_L is proportional to the spectroscopic factor SF_L (see definition, for instance, in [23], [24] and [25], Chapter 9), which play an important role in the theory of nuclear reactions when the Pauli principle is treated approximately [24]. The factor SF_L is used to determine amount of a certain (definite) clusterization in a wave function of the compound system. It is obvious from the definition of the spectroscopic factor (25), that it can be determined for bound state only, when norms of wave functions Ψ_{EL} and ψ_{EL} are finite.

2.1 Definition of basic quantities

Having calculated the wave function of the ground or resonance state in the oscillator representation $C_{nL}^{(E)}$, we can easily construct the inter-cluster wave functions in the coordinate and momentum representations

$$\psi_{EL}(q) = \sum_{n=0} C_{nL}^{(E)} \Phi_{nL}(q, b), \quad (27)$$

$$\psi_{EL}(p) = \sum_{n=0} C_{nL}^{(E)} \Phi_{nL}(p, b). \quad (28)$$

One can use these functions to obtain additional information about bound and resonance states. We will employ wave function of coordinate space $\psi_{EL}(q)$ to calculate an average distance between clusters A_c , which can be defined as

$$A_c = b \sqrt{\langle \psi_{EL}(q) | q^2 | \psi_{EL}(q) \rangle} / \mu, \quad (29)$$

where $\mu = A_1 A_2 / A$ is the reduced mass for selected clusterization. Similarly, we can also determine an average momentum P_c of relative motion of two clusters

$$P_c = b^{-1} \sqrt{\langle \psi_{EL}(p) | p^2 | \psi_{EL}(p) \rangle}. \quad (30)$$

The average momentum P_c is related to an average kinetic energy of two-cluster relative motion by simple relation

$$T_c = \frac{\hbar^2}{2m} P_c^2.$$

By considering continuous spectrum states we will calculate and analyze the weight of internal part of wave function, which we define as

$$W_L(E) = \sum_{n=0}^{N_i-1} \left| C_{nL}^{(E)} \right|^2. \quad (31)$$

This definition of the weight equivalent to following definition

$$W_L(E) = \int_0^R dq q^2 |\psi_{EL}(q)|^2, \quad (32)$$

the radius of internal region R can be determined in self-consistent way as

$$R \approx b\sqrt{4N_i + 2L + 3}.$$

Let us evaluate behavior of function $W_L(E)$ for a simple case when the function $\psi_{EL}(q)$ describes a free motion of two cluster with the orbital momentum $L=0$. Then, the wave function $\psi_E(q) = \psi_{E,L=0}(q)$ is

$$\psi_E(q) = \sqrt{\frac{2}{\pi}} \frac{\sin(kq)}{q},$$

and the weight $W(E)$ is equal to

$$W(E) = \int_0^R dq q^2 |\psi_E(q)|^2 = \frac{2}{\pi} \left[\frac{1}{2}R - \frac{\sin(2kR)}{4k} \right],$$

where k is the wave number

$$k = \sqrt{\frac{2mE}{\hbar^2}}.$$

Thus, in a simple case the weight $W(E)$ as a function of energy has an oscillatory behavior and is decreased with increasing of energy E or wave number k . It is interesting to note that for small values of E we have got

$$W(E) \approx \frac{2}{3\pi} R (kR)^2,$$

the weight $W(E)$ equal zero at $E = 0$, and the slowly increasing as a linear function of energy. Such a behavior of weights as a function of energy suggests that this function has a maximum at relatively small energy. We will see later that the weights $W(E)$ of internal part of scattering wave functions allow us to find position of resonance states and evaluate its width.

Within our method, parameters of resonance states are obtained from corresponding phase shifts by using the Breit-Wigner formula for a phase shift around a resonance state. It assumed that the phase shift δ in the vicinity of a resonance state consists background (potential) phase shift δ_p and resonance phase shift δ_R

$$\delta = \delta_p + \delta_R,$$

where the resonance phase shift is determined by the Breit-Wigner formula

$$\delta_R = -\arctan\left(\frac{\Gamma}{E - E_r}\right).$$

We also assume that the first derivative of the background phase shift with respect to energy is much more smaller than the first derivative of the resonance phase shift with respect to energy. Then, the energy and width of resonance state can be determined from the following equations:

$$\left.\frac{d^2\delta(E)}{dE^2}\right|_{E=E_r} = 0, \quad \Gamma = 2 \left[\left.\frac{d\delta(E)}{dE}\right|_{E=E_r}\right]^{-1}. \quad (33)$$

These relations allows us to determine more correctly the energy and width of a resonance state especially in the case when the background phase shift is not small and when the resonance state is wide.

3 Results and discussion

Before start doing calculations we need to select nucleon-nucleon potential and to fix some parameters. To analyze structure of ^8Be , we selected three semi-realistic nucleon-nucleon potentials which are very often used in many microscopical models of light atomic nuclei. They are the Volkov N2 potential (VP) [26], the Minnesota potential (MP) [27], [28] and modified Hasegawa-Nagata potential (MHNP) [29, 30]. These potentials provide fairly good description of nucleon-nucleon interactions in the states with different values of two-nucleon spin S and isospin T . They also give acceptable energy and size parameters of light nuclei described by a wave function of many-particle shell model. First of all, we have one free parameter in our calculation. It is the oscillator length b . It is natural to choose such value b which minimize the binding energy of an alpha particle. We slightly adjusted the Majorana exchange parameter m in the VP and MHNP, and the exchange parameter u of the MP. The adjusted and original exchange parameters are shown in Table 1. The optimal value of the oscillator length b is also indicated in Table 1.

It is interesting to compare cluster-cluster potential generated by the selected nucleon-nucleon potentials. Unfortunately, it is difficult task since the cluster-cluster potential is nonlocal and energy-dependent interaction. This is due to the Pauli principle. However, we can compare so-called a folding potential which is local and represents the main part of cluster-cluster interaction when the antisymmetrization between clusters is disregarded. It means that in Eq. (1) the antisymmetrization operator $\hat{\mathcal{A}}$ is set to be $\hat{\mathcal{A}} = 1$. In Fig. 1 the folding potentials generated by three nucleon-nucleon potentials are shown as a function

Table 1: Optimal values of oscillator length b and exchange parameter m or u of nucleon-nucleon potentials.

Potential	b , fm	m/u , adjusted	m/u , original
VP	1.376	0.6011	0.600
MP	1.285	0.9347	-
MHNP	1.317	0.3961	0.4057

of the inter-cluster distance. The folding potentials like nucleon-nucleon potentials have the Gaussian shape. However, contrary to nucleon-nucleon potentials, the folding potentials have no repulsive core at small distances between alpha particles. As the folding potential involves the Coulomb interaction of protons, there is a barrier which stipulates existence of the 0^+ resonance state. One can see, that the MP and MHNP generates barrier of the same shape and height.

We start our investigations with the s phase shift of the elastic alpha-alpha scattering and position of the 0^+ resonance state. In Fig. 2 we show behavior of the s phase shift around the 0^+ resonance state. As we can see this example of the classical Breit-Wigner resonance state since phase shift is increased on 180° at the resonance energy and the background phase shift equals zero before and after that energy. We manage to

3.1 Spectrum of resonance states

In Table 2 we compare results of our calculations with the available experimental data [1]. Energy of resonance states is determined with respect to the $\alpha + \alpha$ threshold energy.

There is other way to detect resonance states with small width (i.e. narrow resonance states). This can be done by considering spectrum of two-cluster Hamiltonian as a function of number of oscillator functions involved in calculations. Such dependence is shown in Figures 3 and 4 where spectra of 0^+ and 2^+ state are displayed. By dash-dotted lines we indicated position of the 0^+ and 2^+ resonance states, calculated by using the corresponding phase shifts and equations (33). As we see in Figure 3, energy of the lowest 0^+ state has a plateau exactly at the energy of the 0^+ resonance state. There is no plateau in Figure 4 for the wide 2^+ resonance state. There are only small irregularities in behavior of energy of 2^+ states as a function of number of oscillator functions N . Consequently, such type of figures similar to Figure 3 allows one to predict with very good precision the energy of a very narrow resonance state. This phenomenon is used in the Stabilization Method (see formulation of the method in Ref. [31] and some additional illustrations of the method in [17]) to locate position of resonance states.

In Figure 5 we demonstrate dependence of phase shifts for the alpha-alpha elastic scat-

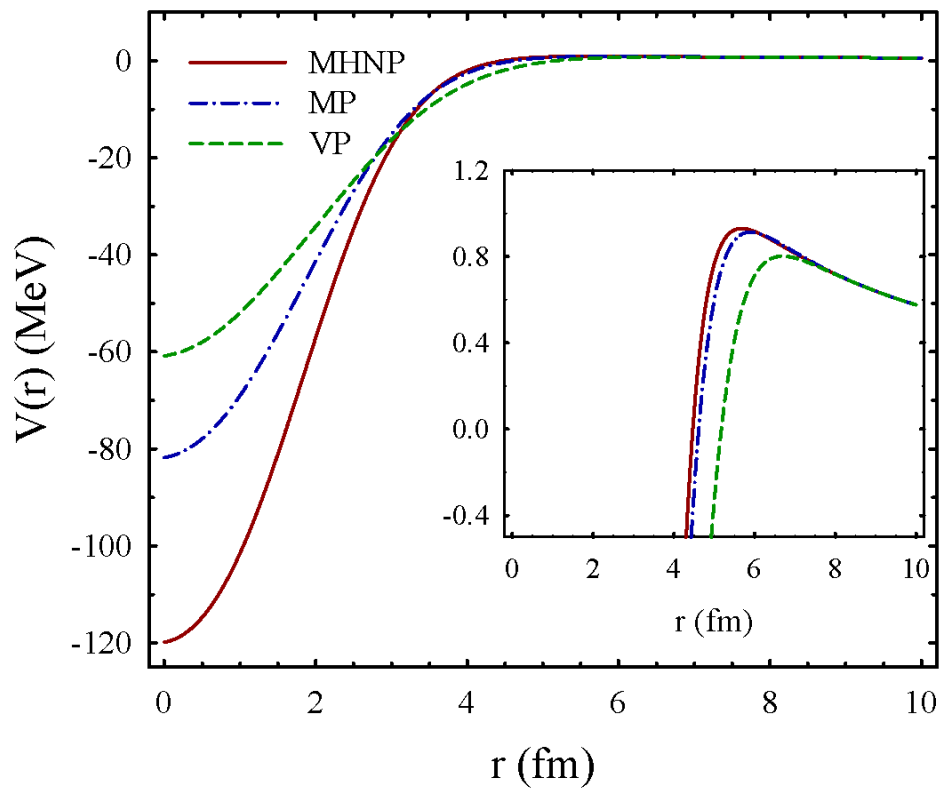


Figure 1: Folding potential of the alpha-alpha interaction generated by the MHNP, MP and VP.

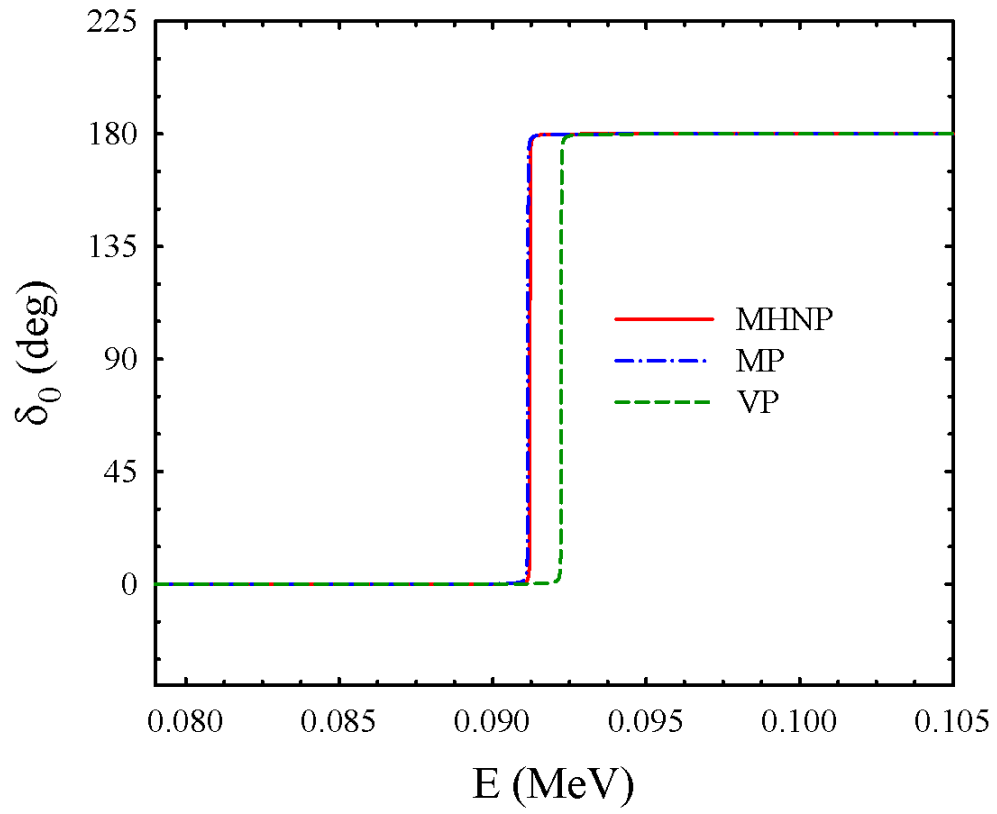


Figure 2: Phase shifts of the alpha-alpha scattering with zero value of the total orbital momentum.

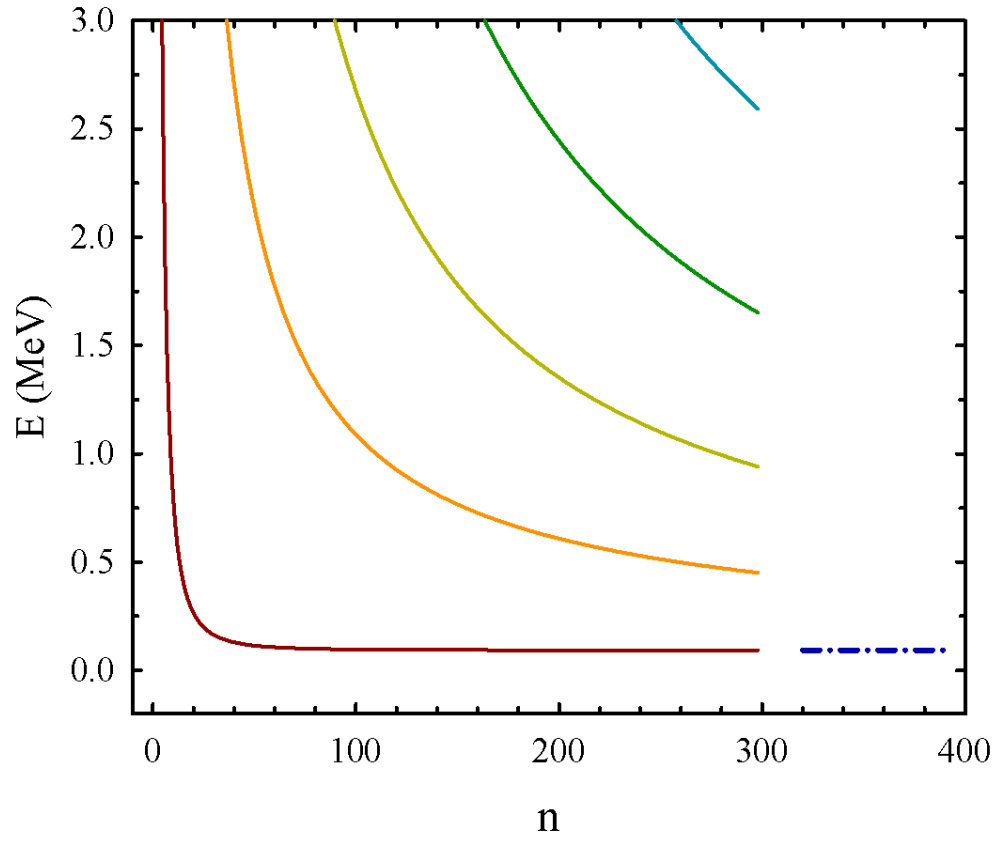


Figure 3: Energy of the 0^+ states of ${}^8\text{Be}$ as a function of number of oscillator functions. Dash-dotted line indicates position of the 0^+ resonance state. Results are obtained with the MHNP.

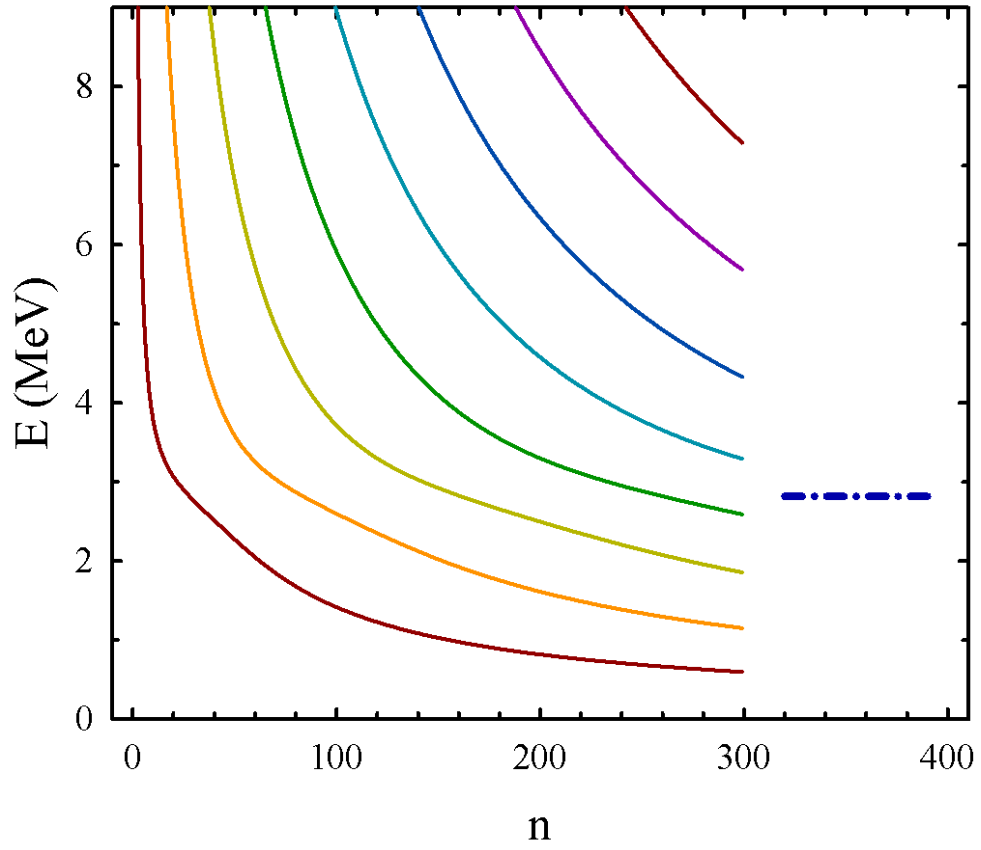


Figure 4: Energy of 2^+ states of ${}^8\text{Be}$ as a function of number of oscillator functions. Dash-dotted line indicates position of the 2^+ resonance state. Results are obtained with the MHNP.

Table 2: Spectrum of resonance states in ^8Be , calculated with three different nucleon-nucleon potentials and compared with experimental data.

L^π	Potential	Theory		Experiment	
		E , MeV	Γ , MeV	E , MeV	Γ , MeV
0^+	MHNP	0.091	$5.183 \cdot 10^{-6}$	0.092	$(5.57 \pm 0.25) \cdot 10^{-6}$
	VP	0.091	$6.947 \cdot 10^{-6}$		
	MP	0.092	$5.876 \cdot 10^{-6}$		
2^+	MHNP	2.818	1.122	3.122 ± 0.010	1.513 ± 0.015
	VP	2.526	1.494		
	MP	2.977	1.773		
4^+	MHNP	10.633	1.816	11.442 ± 0.150	3.500
	VP	10.852	6.732		
	MP	12.710	5.281		

tering on energy and shape of nucleon-nucleon potentials. The S phase shifts calculated with the MHNP and MP are very close in the whole range of energies displayed in Fig. 5. However, the S phase shifts calculated with VP are noticeable different, despite that the VP as the MHNP and MP gives the correct position of the 0^+ resonance state, as it was demonstrated in Table 2. Difference between phases shifts of $\alpha - \alpha$ scattering generated by three potentials is growing with increasing of the total orbital momentum L . This is also reflected on the energy and width of the 2^+ and 4^+ resonance states (see Table 2).

Fig. demonstrates that there is fairly good agreement of our results and experimental data. The experimental data displayed in Fig. 5 are taken from Refs. [32], [33], [34], [35]. One can see that the MHNP and MP potentials yield the 0^+ and 2^+ phase shifts which are very close for experimental data in the presented range of energy. As for the phase shifts with the total orbital momentum 4^+ , our results are close to the experimental data at the energy range $0 \leq E \leq 10$ MeV, and there is deviation from experimental data for all potentials for the energy $E > 10$ MeV.

The weights $W(E)$ of the internal part of scattering wave function introduced in Eq. (32) also reflects existence of resonance state. We demonstrate it for the 2^+ states. The weights displayed in Fig. 6 are calculated with the MHNP (solid line) and with the MP (dot-dashed line). The solid vertical and dot-dashed lines indicates the position of the 2^+ resonance states for the MHNP and MP, respectively. There are two picks in Fig. . The first peak does not connected with resonance state, while the second peak is formed by resonance state. The center of the peak are very close to the energy of the 2^+ resonance state. This figure demonstrates that the weights $W(E)$ as function of energy can confirm existence of

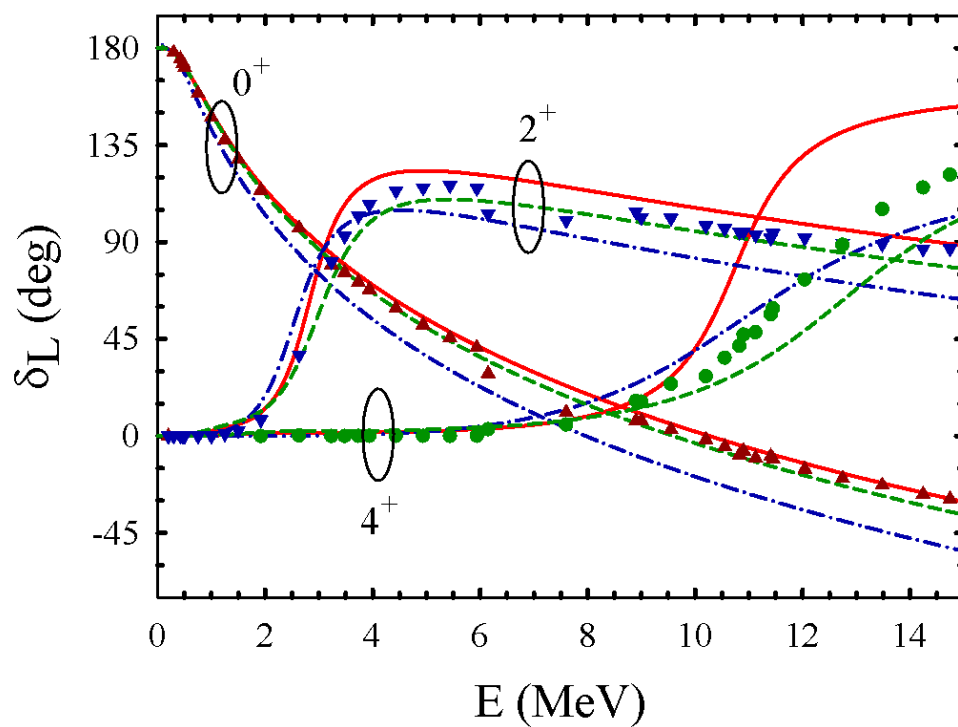


Figure 5: Phase shifts of the elastic $\alpha + \alpha$ scattering calculated with three different NN potentials and compared with experimental data.

rather wide resonance state and indicate of its position.

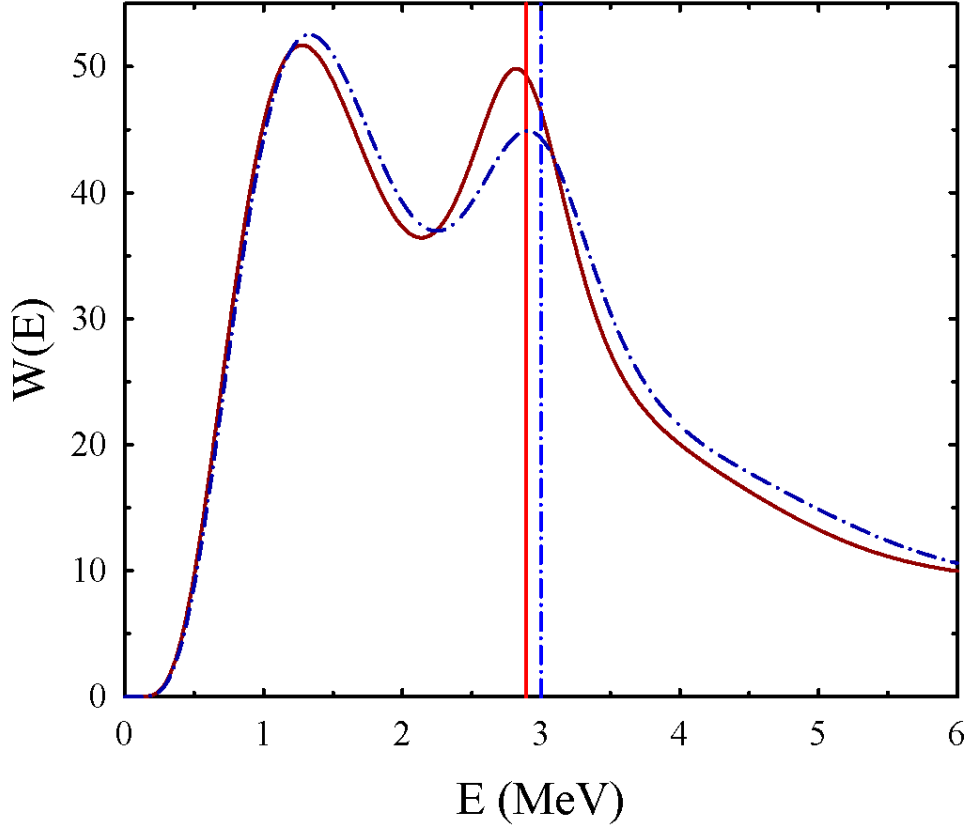


Figure 6: The weights of internal part of scattering wave function as a function of energy constructed for the 2^+ state with the MHNP (solid line) and MP (dot-dashed line). Vertical lines indicate position of the 2^+ resonance states.

3.2 Resonance wave functions

In this section we consider wave functions of resonance states in ${}^8\text{Be}$. We present these functions in oscillator, coordinate and momentum representations. We start with coordinate representations. The wave functions $\psi_{EL}(r)$ of the 0^+ , 2^+ and 4^+ resonance states are displayed in Figure 7. It is interesting to note that maximum of the inter-cluster wave

function of the 0^+ resonance state is at $r = 0$. Thus the Pauli principle allows two alpha particles to be at the same point of the coordinate space. Due to the centrifugal barrier, wave functions of the 2^+ and 4^+ resonance states equal zero at $r = 0$. Other interesting feature of all resonance states is that they have large amplitude of wave function in the internal region ($0 \leq r < 7$ fm) and small amplitude of oscillations in asymptotic region ($r > 7$ fm). Presented results allows us to investigate dependence of resonance wave functions on shape of nucleon-nucleon potential. As we can see in Figure 7, the MHNP and MP give almost identical wave functions for the 0^+ and 2^+ resonance states, but slightly different wave functions for the very broad 4^+ resonance state. Besides, the amplitude of resonance wave functions, calculated with the MHNP and MP, is larger than amplitude of the wave functions, obtained with the Volkov potential.

In Figure 8 we present wave function of the 0^+ , 2^+ and 4^+ resonance states in the oscillator representation. Wave functions of the narrow 0^+ resonance states look like wave function of bound states. Our results confirm conclusion made in Ref. [4], that wave function of narrow resonance states in coordinate or oscillator representations are similar to wave functions of bound states. As we can see, that oscillator functions with $0 \leq n < 20$ dominate in wave functions of all observed resonance states, since expansion coefficients C_n , associated with these functions, have largest weight in resonance wave functions. Resonance wave functions in oscillator representation are similar to corresponding wave functions in coordinate representation: they have large amplitude in the internal region.

Figure 8 demonstrates that the wave functions of the 0^+ and 2^+ resonance states almost independent on shape of nucleon-nucleon potential. The main difference between wave functions of different nucleon-nucleon potentials is observed for the expansion coefficients with very small values of n . As for the wave functions of the 4^+ resonance state, they are very close to the VP and MP potentials, while the wave functions of the resonance states obtained with the MHNP is quite different.

Analysis of results, presented in Figures 7 and 8, shows that the larger is the energy of resonance state, the more oscillations has resonance wave function in coordinate and oscillator representations within the displayed range of variables r and n , respectively.

Wave functions of resonance states in ^8Be are also presented in momentum space (Figure 9). Figure demonstrates that wave functions of 0^+ and 2^+ resonance state are almost independent on the shape of the nucleon-nucleon potential. These wave functions are located in very restricted region of the momentum p . Wave functions of the 4^+ resonance states, obtained with different nucleon-nucleon potentials, are quite different and they spread in more wider region of p . However, they are similar in the range of small values of momentum: $0 \leq p \leq 0.5 \text{ fm}^{-1}$.

To demonstrate that our method is consistent with other alternative methods, we compare our results with results of the Complex Scaling Method (CSM) (recent achievements of

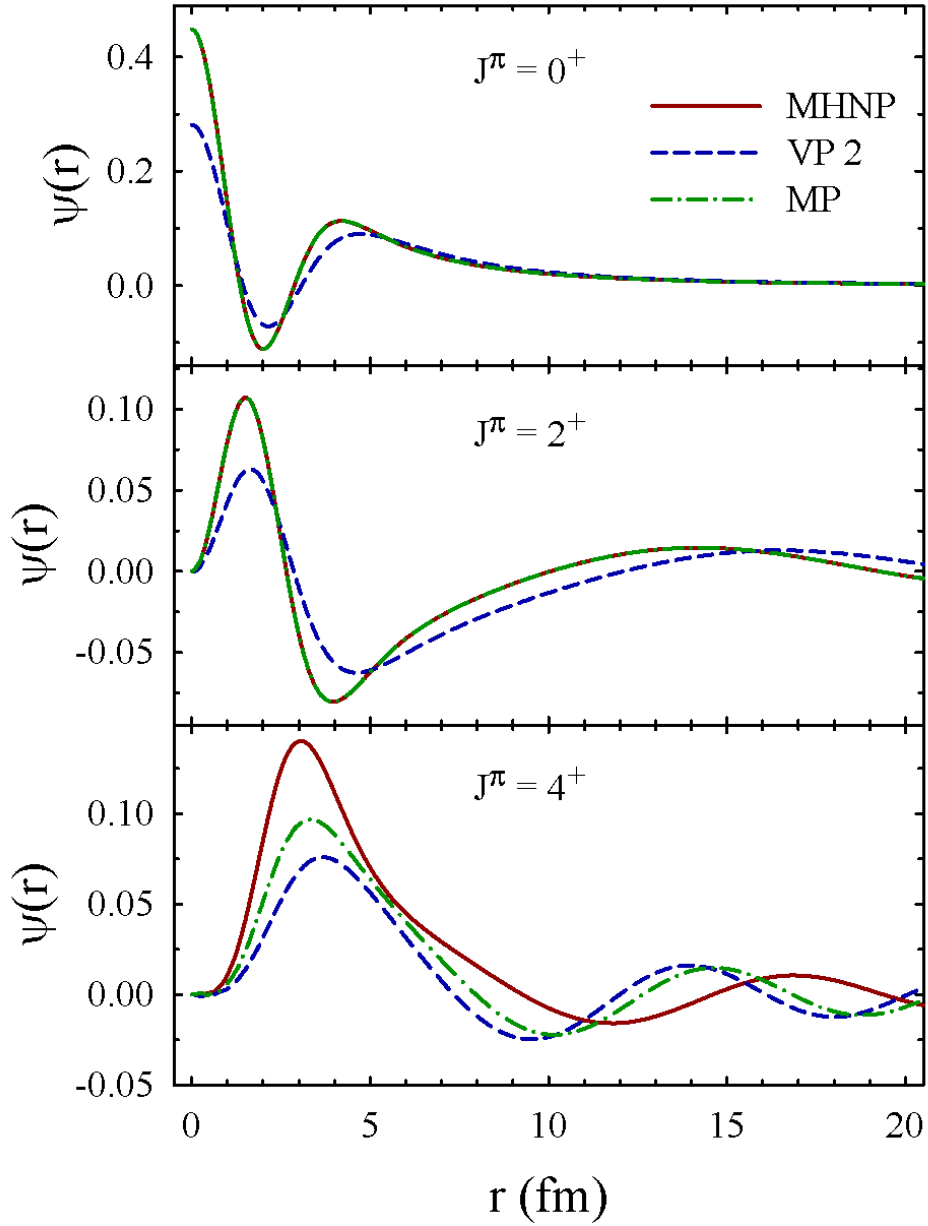


Figure 7: Wave functions of the 0^+ , 2^+ and 4^+ resonance states as a function of distance between alpha particles, calculated with the MHNP, VP and MP potentials.

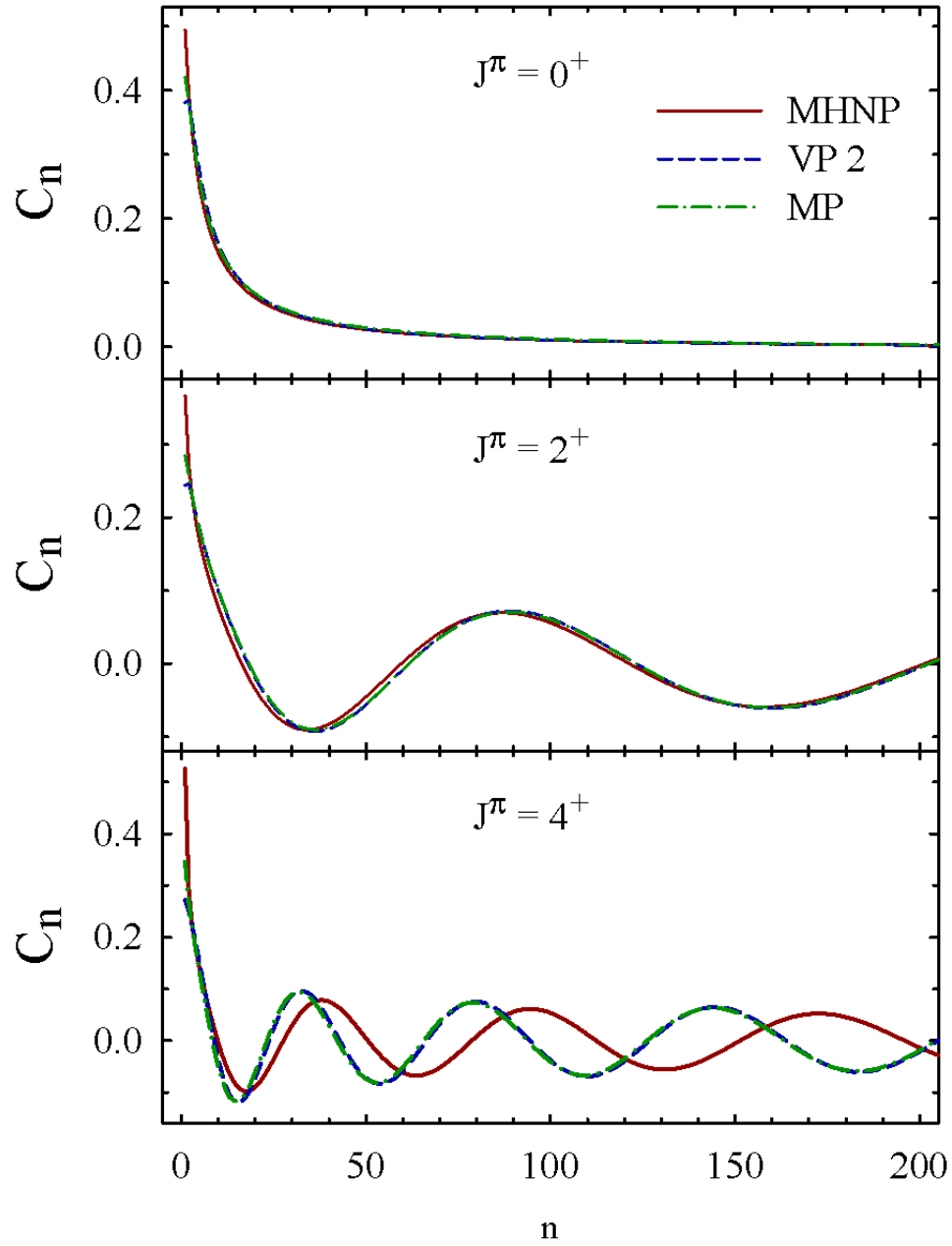


Figure 8: Wave functions of 0^+ , 2^+ and 4^+ resonance states in ${}^8\text{Be}$ in oscillator representation.

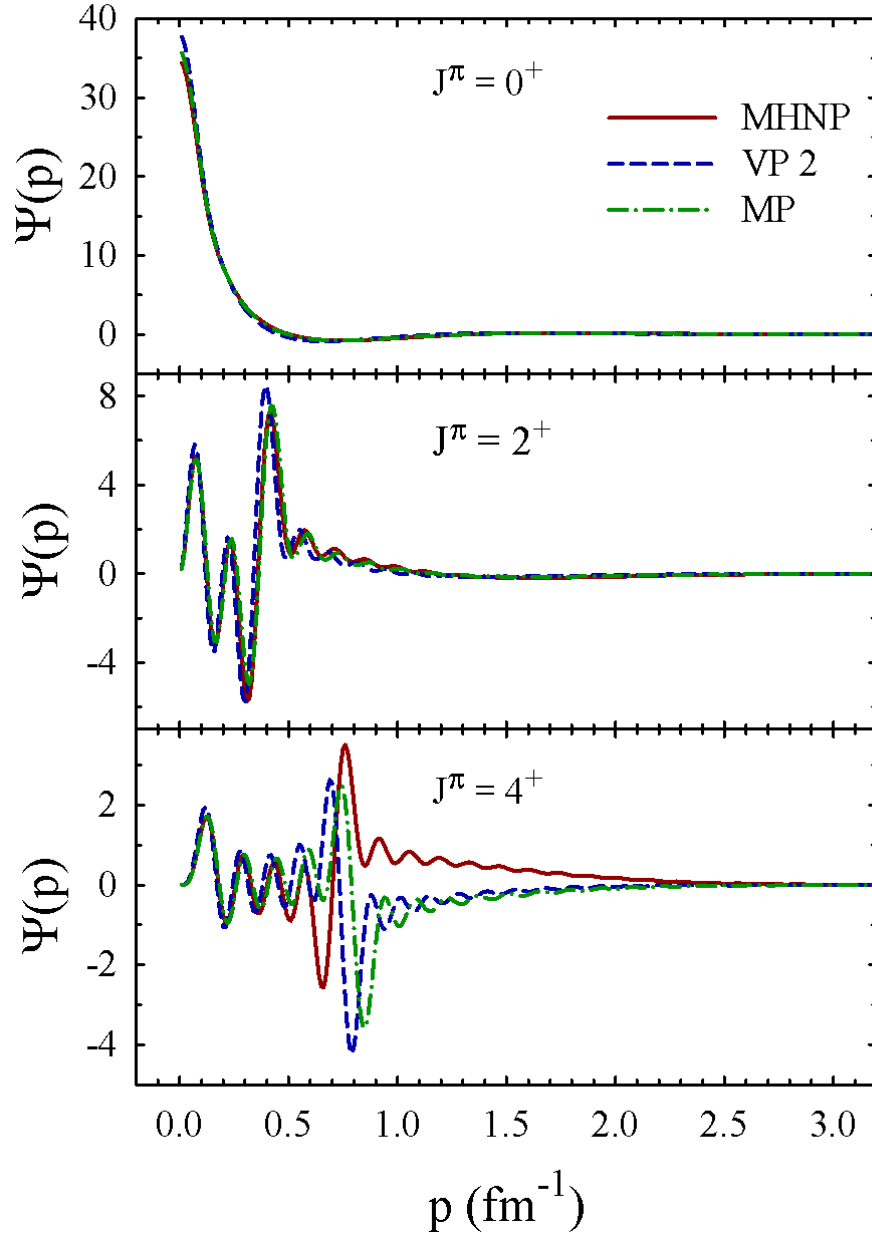


Figure 9: Wave functions of the 0^+ , 2^+ and 4^+ resonance states in ${}^8\text{Be}$ in the momentum space. Results are presented for three NN potentials.

the method and its main ideas can be found in Ref. [36]) which allows one to determine pole of the S -matrix and consequently energy and width of resonance states directly from calculations of eigenvalues of the nonhermitian Hamiltonian. Both calculations are performed with the MHNP and with the same input parameters. Results of these calculations are gathered in Table 3. It is seen that results of our calculations are quite comparable with results of the CSM. The best agreement between two methods is achieved for the 2^+ and 4^+ resonance states, meanwhile energy and width of the 0^+ resonance state are surprisingly different within these methods.

Table 3: Parameters of resonance states calculated within the Resonating Group Method and the Complex Scaling Method.

J^π	Our method		CSM	
	E , MeV	Γ , MeV	E , MeV	Γ , MeV
0^+	0.091	$5.183 \cdot 10^{-6}$	0.150	$35.68 \cdot 10^{-5}$
2^+	2.820	1.196	2.893	1.135
4^+	10.730	1.925	10.824	1.916

It is well-known that the Pauli principle plays an important role in many-body fermion systems and particular in many-cluster systems. The effects have been discussed from a different point of view. We present other way of discussing role of the Pauli principle on wave functions of continuous spectrum states in ^8Be . We calculate and analyze the quantity S_L introduced in Eq. (26). This quantity equals to unity if the Pauli is disregarded or if its effects are negligibly small. Thus, deviation of S_L from unity shows how strong is the effect of the Pauli principle. In Fig. 10 we display S_L as a function of energy for the 0^+ , 2^+ and 4^+ states.

We can see that the largest effect of the Pauli principle is observed for the eigenfunctions whose energy is very close to the energies of detected resonance states. This results reflects the main properties of resonance states, which are the most compact configurations among other states of two-cluster continuum. The smaller is the width of a resonance state, the more compact is its configuration. Fig. 10 demonstrate that the low-energy states ($0 \leq E \leq 50$ MeV) are strongly affected by the Pauli principle than the states with large energy. With increasing of the energy the effects are gradually (steadily) diminished. It is worth noticing that the huge centrifugal barrier in the 4^+ states strongly diminished effects of the Pauli principle for the low-energy states ($0 \leq E \leq 5$ MeV) where $S_J \approx 1$. The centrifugal barrier in 2^+ states is approximately 3 times smaller than in 4^+ states and thus the Pauli principle is stronger for 2^+ states in this range of energy. It is interesting to note that the results shown in Fig. 10 are in agreement with conclusions made in Ref. [4] where two-cluster systems

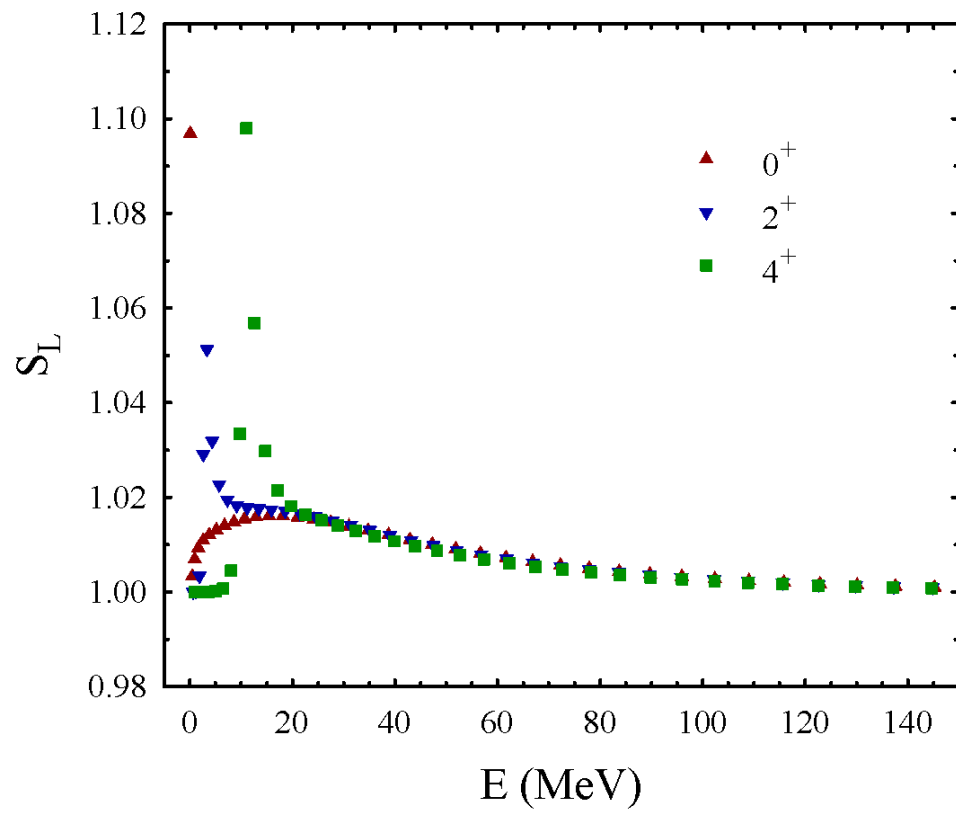


Figure 10: Effects of the Pauli principle in the wave functions of Hamiltonian of ^8Be .

including ${}^8\text{Be}$ have been studied in the Fock-Bargmann representations. This representation is a bridge between quantum-mechanical treatment of nuclear system and classical. It was in particular shown that the classical regime is valid in continuous spectrum of ${}^8\text{Be}$ when energy of such states is larger than 60 MeV. Fig. 10 also shows that effects the Pauli principle in this region is small.

To demonstrate relation between wave function obtained with diagonalization of Hamiltonian with a certain number of oscillator functions and wave function calculated by solving a set of linear equations (5) with necessary boundary conditions, we used the following procedure. First, we diagonalize 250×250 matrix of Hamiltonian for the 2^+ state and select an eigenstate with the energy close to the energy of 2^+ resonance states. Thus we selected the four eigenfunction with the energy $E_4=2.929$ MeV. This function we mark as function D, as it was obtained with the diagonalization. Second, we solved the system of linear algebraic equations with the energy very close to the energy of the four eigenstates. We employ 400 oscillator functions to show behavior of expansion coefficients in a large range of index n . The wave function calculated in such way is marked by liter L. As they normalized in different ways, we renormalize wave function L to make comparison self-consistent. We divided wave function L $\{C_{nL}^{(E)}\}$ on the square root of the sum S_{250}

$$S_{250} = \sum_{n=0}^{249} |C_{nL}^{(E)}|^2$$

As the results part of wave function L represented by 250 oscillator functions is normalized in the same way as function D. Renormalized wave function L and wave function D are demonstrated in Fig. 11. There is small difference for the expansion coefficients with small values of n , which owned to small difference of energy of D and L states. In a large range of n they are very close to each other. Wave function L can be easily extended to very large values n ($n \lesssim 400$) since we know an asymptotic behavior of the function.

We select the wave function of 2^+ state which is displayed in Fig. 11 and obtained from diagonalization procedure, to show the relation between coordinate wave function and expansion coefficients discussed above and presented in Eq. (20). Fig. 12 visualize such relation. We can see that all expansion coefficients starting from $n = 4$ are very close to the wave function in coordinate space. This figure confirms once more that there is simple connection between coordinate and oscillator representations. This connection is valid not only for large values of index n as it was deduced originally, but also a fairly small values.

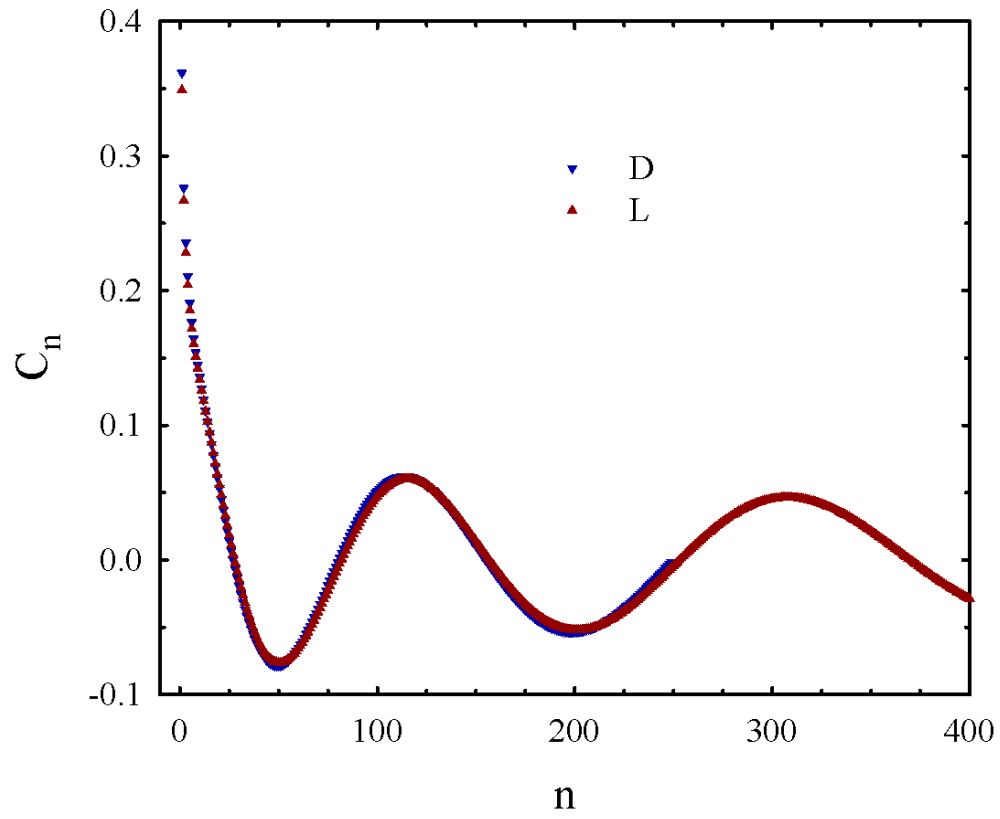


Figure 11: Wave functions of the 2^+ state obtained with diagonalization of Hamiltonian (D) and by solving system of linear algebraic equations (L).

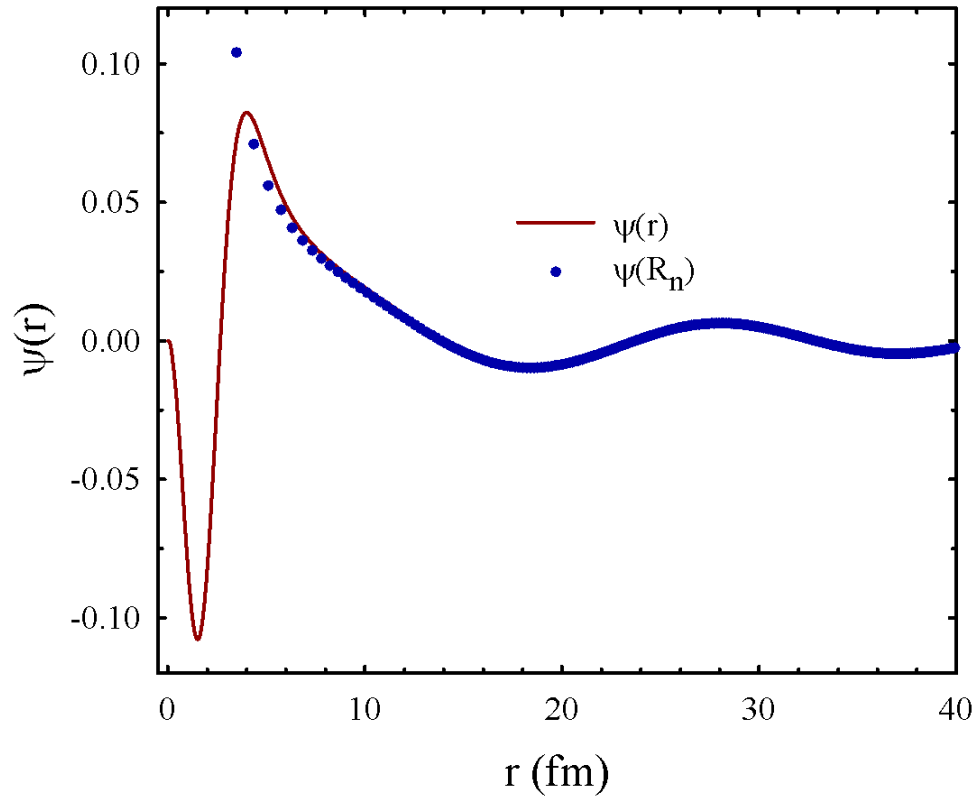


Figure 12: Wave function $\psi(r)$ of the $2+$ state with the energy $E=2.92$ MeV as function of inter-cluster distance (solid line) and expansion coefficients ($\psi(R_n)$) of the function as a function of discrete distance R_n .

Table 4: The mass root-mean-square radii and average distances between alpha particles for some pseudo-bound 0^+ , 2^+ and 4^+ states.

$L^\pi = 0^+$			$L^\pi = 2^+$			$L^\pi = 4^+$		
E , MeV	R_m , fm	A_c , fm	E , MeV	R_m , fm	A_c , fm	E , MeV	R_m , fm	A_c , fm
0.091	3.11	6.35	0.610	11.31	22.62	6.44	9.67	19.35
0.462	10.74	21.48	1.168	10.14	20.28	8.07	9.44	18.88
0.953	10.01	20.02	1.876	9.49	18.99	9.71	8.62	17.25
1.664	9.89	19.78	2.624	8.25	16.51	11.03	7.59	15.24
2.604	9.84	19.69	3.329	8.32	16.67	12.60	8.93	17.87

3.2.1 Average distances between clusters

In Table 4 we display energy of obtained by diagonalizing Hamiltonian, mass root-mean-square (rms) radii R_m of ${}^8\text{Be}$ in these states, and average distance A_c between clusters. These results are obtained with MHNP. It is necessary to point out that the most compact configurations of ${}^8\text{Be}$ are revealed in those eigenstates of Hamiltonian whose energies are very close to the energy of resonance states. They are the first state for $L^\pi = 0^+$ and the fourth state for $L^\pi = 2^+$. These two states have the smallest mass rms radius and smallest average distance between alpha particles. As we can see, the average distances are approximately two times larger than corresponding mass rms radii. It is also worth noticing that the low-energy states (except the 0^+ resonance state) have largest distance between alpha-particles. Thus the low-energy states in a cluster model are very dispersed (stretched) states. This is stipulated by the shape of their wave functions which dominantly represented by oscillator functions with large values of the index n .

In Table 4 we display five 0^+ and 2^+ states with the lowest energies, while for the 4^+ states we selected those eigenstates which are close to the energy of the 4^+ resonance state. Results presented in Table 4 show effects of the Pauli principle on restricted set of eigenstates. The full picture of the effects for a large range of states are displayed in Figs. 13 and 14. In Fig. 13 we show for the 0^+ states the mass rms radii R_m , the average distance between alpha clusters A_c and the average momentum P_c as function of energy. The same information is displayed in Fig. 14 for the 0^+ states.

The average distances between an interacting clusters has been discussed in literature where cluster models are applied to study different nuclear hypernuclear system. For example, in Ref. [37] the hypernucleus ${}^9_\Lambda\text{Be}$ has been studied within a three-cluster model with the partition $\alpha + \alpha + \Lambda$. The nucleus ${}^8\text{Be}$ comprised by two alpha particles is a major ingredient of the model. An approximate formula was used in Ref. [37] to extract the average $\alpha - \alpha$ distance. Recall that we use a rigorous way for obtaining this quantity. The average distance

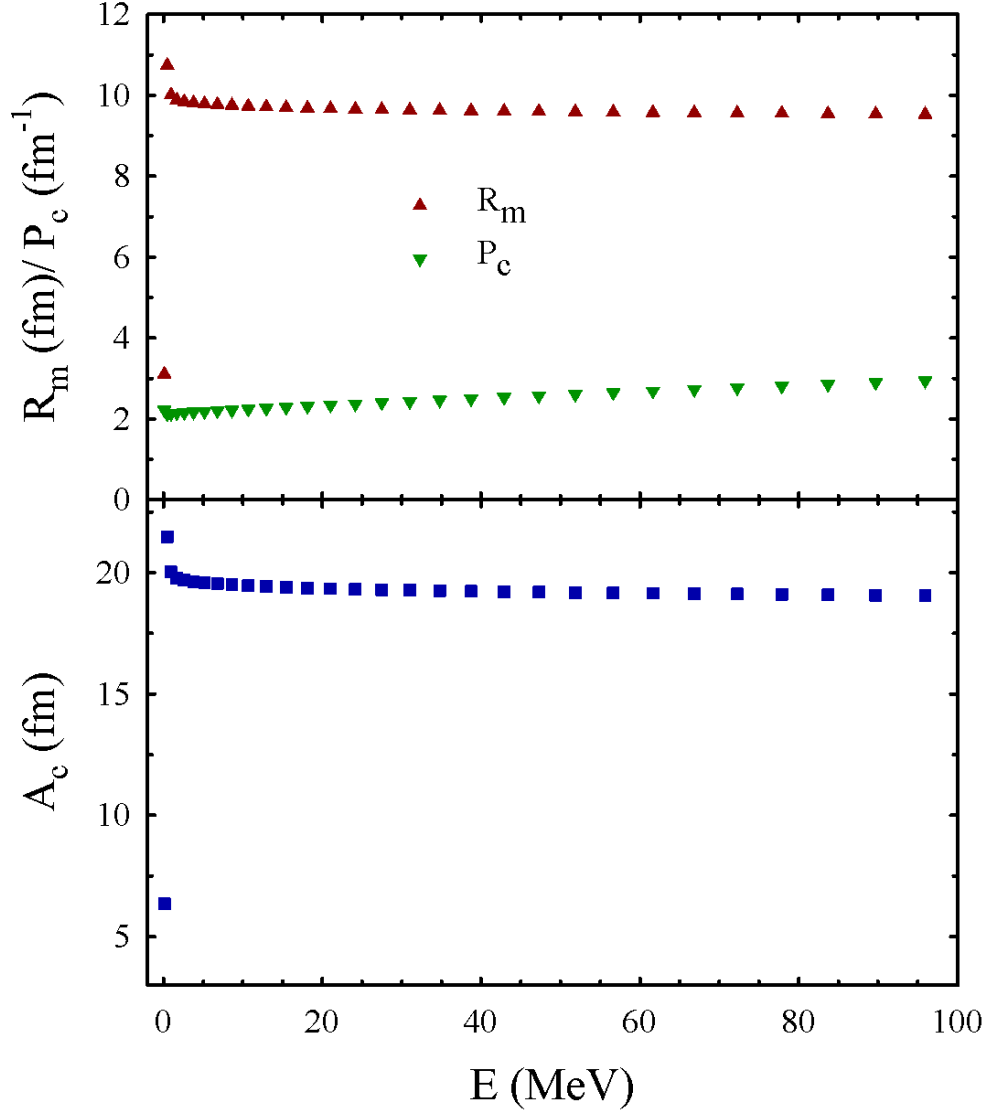


Figure 13: The mass rms radius R_m , the average distance between alpha clusters A_c and the average momentum of their relative motion P_c as a function of energy obtained for the 0^+ states with the MHNP.

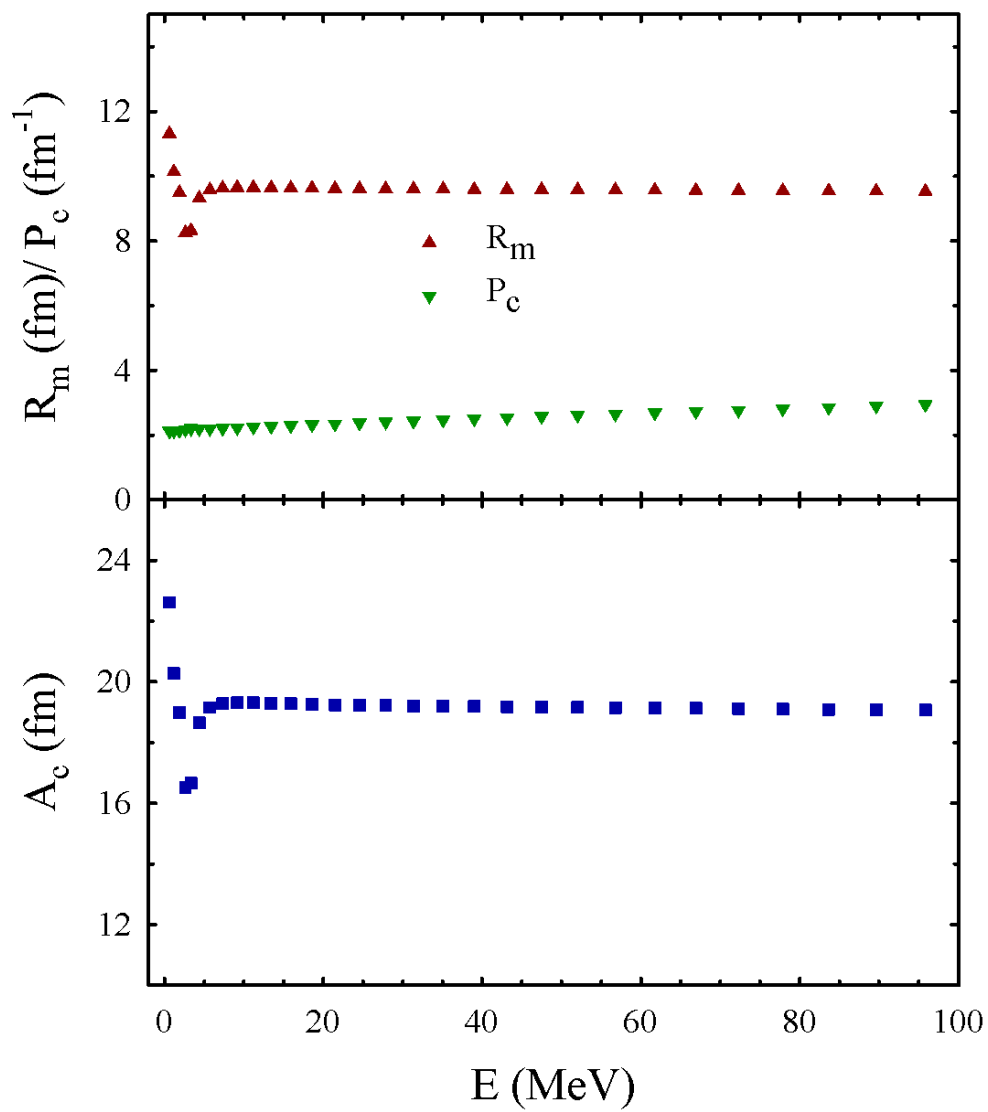


Figure 14: The same as in Fig. 13 but for the states with $J^\pi=2^+$

between alpha particles was evaluated to be 5.99 fm in the ground 0^+ state which is close to our evaluation $A_c = 6.35$ fm.

4 Conclusions

We have applied a two-cluster microscopic model for investigation of alpha-alpha scattering and resonance structure of ^8Be . The model is the resonating group method with a matrix form of dynamic equations. Transition from coordinate form to the matrix form was implemented with the help of oscillator functions. Three popular semi-realistic nucleon-nucleon potentials were involved in calculations to determine both the internal energy of each cluster and interaction between them. They also determine dynamics of alpha-alpha scattering and resonance structure of ^8Be . These potentials were used to study dependence of spectrum, phase shifts and wave functions of different states on the shape of nucleon-nucleon potential. Small tuning of parameters of nucleon-nucleon potentials allowed us to reproduce with a good accuracy the energy and width of the 0^+ resonance state. The same parameters of potentials were used to calculate 0^+ , 2^+ and 4^+ phase shifts of elastic alpha-alpha scattering and the position of 2^+ and 4^+ . Our results are in a fairly good agreement with available experimental data and with results of other microscopical models.

It was shown that the Pauli principle has largest impact on the wave functions of resonance states, since resonance states are the most compact two-cluster configurations among other states of continuous spectrum. This was confirmed by calculations of the mass root-mean-square radius and average distance between alpha-particles. These calculations were performed within large but finite set of oscillator functions. It was also demonstrated that the effects of the Pauli principle are steadily decreasing with increasing of energy of ^8Be .

5 Acknowledgment

This work was supported in part by the Program of Fundamental Research of the Physics and Astronomy Department of the National Academy of Sciences of Ukraine (Project No. 0117U000239) and by the Ministry of Education and Science of the Republic of Kazakhstan, Research Grant IRN: AP 05132476.

References

- [1] D. R. Tilley, J. H. Kelley, J. L. Godwin, D. J. Millener, J. E. Purcell, C. G. Sheu, and H. R. Weller, "Energy levels of light nuclei $A=8, 9, 10$," *Nucl. Phys. A*, vol. 745,

- pp. 155–362, 2004.
- [2] G. F. Filippov and I. P. Okhrimenko, “Use of an oscillator basis for solving continuum problems,” *Sov. J. Nucl. Phys.*, vol. **32**, pp. 480–484, 1981.
 - [3] G. F. Filippov, “On taking into account correct asymptotic behavior in oscillator-basis expansions,” *Sov. J. Nucl. Phys.*, vol. **33**, pp. 488–489, 1981.
 - [4] Y. A. Lashko, G. F. Filippov, and V. S. Vasilevsky, “Dynamics of two-cluster systems in phase space,” *Nucl. Phys. A*, vol. 941, pp. 121–144, 2015.
 - [5] A. S. Solovyev, S. Y. Igashov, and Y. M. Tchuvil’sky, “Radiative Capture Processes in Multi-Size-Scale Algebraic Version of Resonating Group Model,” *J. Phys. Conf. Ser.*, vol. 863, p. 012015, 2017.
 - [6] A. S. Solovyev, S. Y. Igashov, and Y. M. Tchuvil’sky, “Treatment of the Mirror ${}^3\text{H}(\alpha, \gamma){}^7\text{Li}$ and ${}^3\text{He}(\alpha, \gamma){}^7\text{Be}$ Reactions in the Algebraic Version of the Resonating Group Model,” *J. Phys. Conf. Ser.*, vol. 569, p. 012020, 2014.
 - [7] V. S. Vasilevsky, K. Katō, V. Kurmangaliyeva, A. D. Duisenbay, N. Kalzhigitov, N. Takibayev, Investigation of discrete and continuous spectrum states in two-cluster system. Sapporo, Japan: Hokkaido University, 2017.
 - [8] A. D. Duisenbay and N. Zh. Takibayev and V. S. Vasilevsky and V. O. Kurmangaliyeva and E. M. Akzhigitova, “Form factors and density distributions of protons and neutrons in ${}^7\text{Li}$ and ${}^7\text{Be}$,” *News Nat. Acad. Scien. Rep. Kazakhstan*, vol. 3, no. 325, pp. 71–76, 2019.
 - [9] A. V. Nesterov, F. Arickx, J. Broeckhove, and V. S. Vasilevsky, “Three-cluster description of properties of light neutron- and proton-rich nuclei in the framework of the algebraic version of the resonating group method,” *Phys. Part. Nucl.*, vol. 41, pp. 716–765, 2010.
 - [10] V. S. Vasilevsky, K. Katō, and N. Takibayev, “Systematic investigation of the hoyle-analog states in light nuclei,” *Phys. Rev. C*, vol. 98, p. 024325, 2018.
 - [11] V. S. Vasilevsky, N. Takibayev, and A. D. Duisenbay, “Microscopic description of ${}^8\text{Li}$ and ${}^8\text{B}$ nuclei within three-cluster model,” *Ukr. J. Phys.*, vol. 62, no. 6, pp. 461–472, 2017.

- [12] A. D. Duisenbay, N. Kalzhigitov, K. Katō, V. O. Kurmangaliyeva, N. Takibayev, and V. S. Vasilevsky, “Effects of the Coulomb interaction on parameters of resonance states in mirror three-cluster nuclei,” *Nucl. Phys. A*, vol. 996, p. 121692, 2020.
- [13] M. Abramowitz and A. Stegun, *Handbook of Mathematical Functions*. New-York: Dover Publications, Inc., 1972.
- [14] G. F. Filippov, L. L. Chopovsky, and V. S. Vasilevsky, “On ${}^7\text{Li}$ resonances in the $\alpha + t$ channel,” *Sov. J. Nucl. Phys. (Yad. Fiz.)*, vol. 37, no. 4, pp. 839–846, 1983.
- [15] H. A. Yamani and L. Fishman, “J-matrix method: Extensions to arbitrary angular momentum and to Coulomb scattering,” *J. Math. Phys.*, vol. 16, pp. 410–420, 1975.
- [16] E. J. Heller and H. A. Yamani, “New L^2 approach to quantum scattering: Theory,” *Phys. Rev.*, vol. A9, pp. 1201–1208, 1974.
- [17] G. F. Filippov, V. S. Vasilevsky, and L. L. Chopovsky, “Solution of problems in the microscopic theory of the nucleus using the technique of generalized coherent states,” *Sov. J. Part. Nucl.*, vol. 16, pp. 153–177, 1985.
- [18] A. I. Baz and Ya. B. Zel’dovich and A. M. Perelomov, *Scattering, Reaction in Non-Relativistic Quantum Mechanics*. Jerusalem: Israel Program for Scientific Translations, 1969.
- [19] R. G. Newton, *Scattering Theory of Waves and Particles*. New-York: McGraw-Hill, 1966.
- [20] H. A. Yamani and L. Fishman, “J - matrix method: Extensions to arbitrary angular momentum and to Coulomb scattering,” *J. Math. Phys.*, vol. 16, pp. 410–420, 1975.
- [21] Y. I. Nechaev and Y. F. Smirnov, “Solution of the scattering problem in the oscillator representation,” *Sov. J. Nucl. Phys.*, vol. 35, pp. 808–811, 1982.
- [22] N. Kalzhigitov and N. Zh. Takibayev and V. S. Vasilevsky, E. M. Akzhigitova and V. O. Kurmangaliyeva, “A microscopic two-cluster model of processes in ${}^6\text{Li}$,” *News Nat. Acad. Scien. Rep. Kazakhstan*, in press, 2020.
- [23] M. H. Macfarlane and J. B. French, “Stripping Reactions and the Structure of Light and Intermediate Nuclei,” *Rev. Mod. Phys.*, vol. 32, pp. 567–691, 1960.
- [24] Norman K Glendenning, *Direct nuclear reactions*. Singapore: World Scientific, 1983.

- [25] O. F. Nemets, V. G. Neudachin, A. T. Rudchik, Yu. F. Smirnov and Yu. M. Tchuvil'sky, *Nucleon Clusters in Atomic Nuclei and Many-Nucleon Transfer Reactions. (in Russian)*. Kiev: 'Naukova Dumka', 1988.
- [26] A. B. Volkov, "Equilibrium deformation calculation of the ground state energies of 1p shell nuclei," *Nucl. Phys.*, vol. **74**, pp. 33–58, 1965.
- [27] D. R. Thompson, M. LeMere, and Y. C. Tang, "Systematic investigation of scattering problems with the resonating-group method," *Nucl. Phys.*, vol. **A286**, no. 1, pp. 53–66, 1977.
- [28] I. Reichstein and Y. C. Tang, "Study of $N+\alpha$ system with the resonating-group method," *Nucl. Phys. A*, vol. 158, pp. 529–545, 1970.
- [29] A. Hasegawa and S. Nagata, "Ground state of ${}^6\text{Li}$," *Prog. Theor. Phys.*, vol. 45, pp. 1786–1807, 1971.
- [30] F. Tanabe, A. Tohsaki, and R. Tamagaki, " $\alpha\alpha$ scattering at intermediate energies," *Prog. Theor. Phys.*, vol. 53, pp. 677–691, 1975.
- [31] A. U. Hazi and H. S. Taylor, "Stabilization Method of Calculating Resonance Energies: Model Problem," *Phys. Rev. A*, vol. 1, pp. 1109–1120, 1970.
- [32] N. P. Heydenburg and G. M. Temmer, "Alpha-Alpha Scattering at Low Energies," *Phys. Rev.*, vol. 104, pp. 123–134, 1956.
- [33] T. A. Tombrello and L. S. Senhouse, "Elastic Scattering of Alpha Particles from Helium," *Phys. Rev.*, vol. 129, pp. 2252–2258, 1963.
- [34] P. Darriulat, G. Igo, H. G. Pugh, and H. D. Holmgren, "Elastic Scattering of Alpha Particles by Helium Between 53 and 120 MeV," *Phys. Rev.*, vol. 137, pp. 315–325, Jan. 1965.
- [35] W. S. Chien and R. E. Brown, "Study of the $\alpha+\alpha$ system below 15 MeV (c.m.)," *Phys. Rev. C*, vol. 10, pp. 1767–1784, 1974.
- [36] T. Myo, Y. Kikuchi, H. Masui, and K. Katō, "Recent development of complex scaling method for many-body resonances and continua in light nuclei," *Progr. Part. Nucl. Phys.*, vol. 79, pp. 1–56, 2014.
- [37] Y. Kanada-En'yo, "Excitation energy shift and size difference of low-energy levels in p -shell Λ hypernuclei," *Phys. Rev. C*, vol. 97, p. 024330, 2018.